International Journal of Heat and Mass Transfer 52 (2009) 1070–1074

Contents lists available at ScienceDirect

International Journal of Heat and Mass Transfer

journal homepage: www.elsevier.com/locate/ijhmt

Technical Note

An experimental and numerical study of forced convection in a microchannel with negligible axial heat conduction

Guodong Wang, Liang Hao, Ping Cheng *

Ministry of Education Key Laboratory of Power Machinery and Engineering, School of Mechanical and Power Engineering, Shanghai Jiaotong University, Shanghai 200240, PR China

ARTICLE INFO

Article history:
Received 1 June 2008
Received in revised form 24 June 2008
Available online 31 August 2008

Keywords:
Heat transfer
Laminar flow
Microchannel
Microheater
Numerical simulation

ABSTRACT

Experiments are conducted for laminar forced convection of water in a microchannel under partially-heated and fully-heated conditions on one wall with negligible axial heat conduction. The microchannel had a trapezoidal cross-sectional shape, with a hydraulic diameter of 155 μm and a heating length of 30 mm. Three-dimensional numerical simulations, based on the Navier–Stokes equations and energy equation, are obtained for forced convection of water in this microchannel under the same experimental conditions. It is found that the numerical predictions of wall temperatures and local Nusselt numbers are in good agreement with experimental data. This confirms that classical Navier–Stokes and energy equations are valid for the modeling of convection in a microchannel having a hydraulic diameter as small as 155 μm. For a microchannel with the same cross-sectional shape with one-wall heated and a heating length of 100 mm, numerical results show that the thermal entrance length is given by $z = 0.15 Re Pr D_h$, with the fully-developed Nusselt number approaching a constant value of 4.00.

1. Introduction

In early 1980 s, Tuckerman and Pease [1] performed an experiment showing that extraordinarily high convective heat transfer coefficient could be achieved in forced convection of water in microchannels. Since that time, many experimental and numerical studies [2–8] have been carried out to study forced convection in microchannel heat sinks because of its potential applications for cooling of high-performance microprocessors, laser diode arrays, and high-energy-laser mirrors.

However, the Nusslet numbers, determined from previous experimental studies [2–4] on forced convection in silicon microchannels under constant heat flux, were not comparable with each other. Numerical studies [5–8] showed that axial heat conduction on the wall was important in forced convection in silicon microchannels. In particular, Li et al. [8] conducted a numerical simulation for forced convection of water in silicon-based microchannel heat sinks, and found that approximately 40–60% of the heat flux (at $Re = 40$) supplied to the heat sink was conducted from downstream part into the upstream part of the highly conducting silicon substrate. Thus, it appears that the non-uniform heat flux distribution from the wall to the coolant along the microchannels may be one of the reasons why different investigators obtained different Nusselt numbers in their experimental studies of forced convection in silicon/copper based microchannels.

In this paper, we have performed an experimental study on forced convection of water in a microchannel having a hydraulic diameter of 155 μm with a heating length of 30 mm with negligible axial heat conduction on the wall for the cases of partially-heated and fully-heated conditions. Numerical solutions corresponding to experimental conditions were obtained, and results of wall temperature distribution and local Nusselt number are compared with experimental data. The good agreement of numerical predictions and experimental data confirms that Navier–Stokes equations are applicable for modeling of forced convection in a microchannel with a hydraulic diameter as small as 155 μm. Numerical simulation for a fictitious microchannel with the same cross-sectional shape but with a heating length extended to 100 mm was also performed to obtain the Nusselt number of a thermally fully-developed forced convective flow in a microchannel.

2. Description of the experiment and numerical simulation

2.1. Experimental setup

Fig. 1 shows the experimental apparatus and the flow circuit of the present experiment, which was used in our previous paper for flow boiling in microchannels [9]. It consisted of a working fluid loop, a test section integrated with microheaters, and a data acquisition system. The deionized water flowed successively through a degassing unit, a constant temperature bath, a filter, a needle valve and finally the test section. Fifteen microheaters, serving also as

* Corresponding author.
E-mail address: pingcheng@sjtu.edu.cn (P. Cheng).

0017-9310/$ - see front matter © 2008 Elsevier Ltd. All rights reserved.
doi:10.1016/j.ijheatmasstransfer.2008.06.038

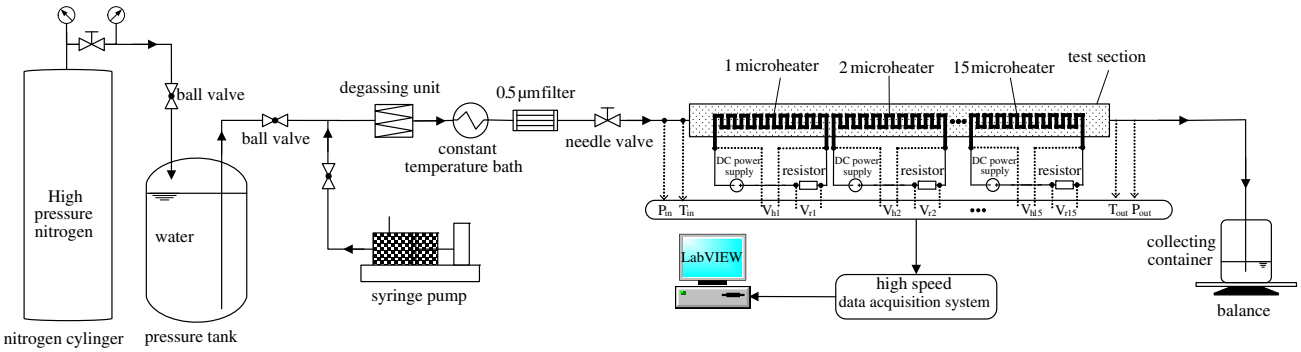

Fig. 1. Experimental test loop.

temperature sensors, were connected with fifteen DC power supplies separately. The average temperature of the microheater was determined from R_h according to the relationship between resistance and temperature of platinum. All signals of pressure, temperature and voltage of the microheaters were collected by a NI high-speed data acquisition system.

The microchannel was etched in a ⟨100⟩ silicon substrate bonded from the top and bottom by two Pyrex glass plates. The microchannel, 427 μm in the top width, 276 μm in bottom width and 107 μm in depth, had a hydraulic diameter of 155 μm with a heating length of 30 mm (see Fig. 2). Fifteen identical platinum microheaters (numbered from #1 to #15 in the flow direction) were sputtered on the bottom Pyrex glass wall. Since the Pyrex glass substrate had a very low thermal conductivity (0.66 W/m K) compared with silicon (148 W/m K) or copper (398 W/m K), it ensured that axial heat conduction in the bottom wall was negligibly small.

The total heat flux supplied to the microheater q and the effective heat flux absorbed by the fluid q_{eff} were calculated according to:

$$q = V_h I/A \quad \text{and} \quad q_{eff} = q - q_{loss} \tag{1a, b}$$

where V_h and I are the voltage and current of the microheater, and A is the area of the microheater. The conduction heat loss q_{loss} from the test section was determined from a heat conduction experiment at stationary fluid condition prior to convection experiments. In the forced convection experiment, the maximum heat loss was less than 10% of the total heat supplied. The Nusselt number on each microheater determined from the experiment is calculated from

$$Nu(z) = \frac{q_{eff} \cdot D_h}{k \cdot \Delta T(z)} \tag{2}$$

where D_h is hydraulic diameter of the microchannel, k the thermal conductivity of water, q_{eff} the effective heat flux given by Eq. (1b), and $\Delta T(z) = T_w(z) - T_l$ with T_w being the microheater temperature and T_l the bulk temperature of water which was calculated from $T_l = (T_{out} + T_{in})/2$ where T_{in} and T_{out} being the inlet and outlet temperatures of water, respectively. The measurement errors of D_h, q_{eff}, ΔT_b and $k(T)$ were estimated to be 1.8%, 2.6%, .2.9%, and 1.0%, respectively, and the maximum uncertainty in determining Nu was 8.3%.

2.2. Description of numerical simulation

The Navier–Stokes and energy equations are used to model the convective heat transfer process with the following assumptions: (i) steady 3D fluid flow and heat transfer; (ii) laminar flow and incompressible fluid; (iii) physical properties of water, such as thermal conductivity, density, and specific heat are temperature dependent; and (iv) negligible radiation heat transfer. According to the above assumptions, the 3D governing equations are:

$$\text{Continuity}: \quad \nabla \cdot (\rho_l \vec{U}) = 0 \tag{3}$$

$$\text{Momentum}: \quad \nabla \cdot (\rho_l \vec{U}\overline{U}) = -\nabla P + \nabla \cdot (\mu_l \nabla \overline{U}) \tag{4}$$

$$\text{Energy}: \quad \nabla \cdot (\rho_l \vec{U}T) = \nabla \cdot \left(\frac{k_l}{C_{p,l}} \nabla T \right) \tag{5}$$

No-slip boundary conditions are imposed on the walls of the microchannels. At the inlet, mass flux and temperature are specified. At the outlet, pressure is specified and temperature gradient is assumed to be zero. A uniform heat flux condition q_{eff} is imposed over the microheater on the Pyrex wall, and the heat flux is zero at all other walls. After numerical solutions for Eqs. (3)–(5) with the aforementioned boundary conditions have been carried out, the

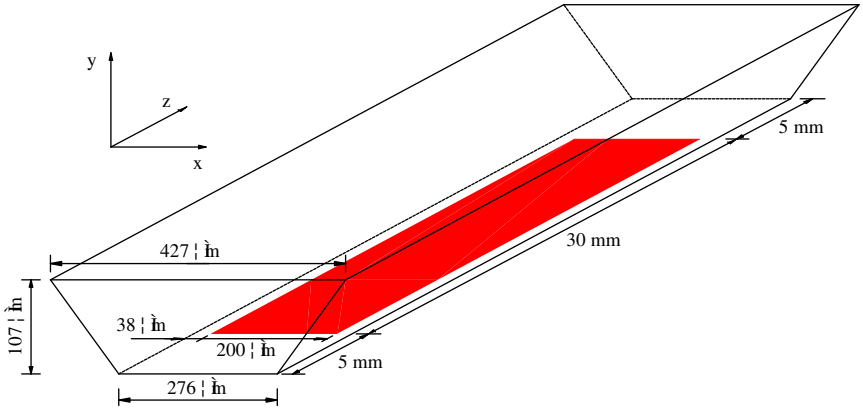

Fig. 2. Sketch of numerical simulation domain for a microchannel with one wall fully-heated.

local Nusselt number is computed according to Eq. (2) where $\Delta T(z) = T_{w,\Gamma}(z) - T_l(z)$. Here, $T_{w,\Gamma}(z)$ is the local averaged inner heating wall temperature and $T_l(z)$ is the cross-sectional averaged bulk temperature, which can be calculated, respectively, from

$$T_{w,\Gamma}(z) = \frac{\sum_\Gamma T_{w,\Gamma}(i,j,k)}{N_\Gamma} \tag{6}$$

where N_Γ is the total number of node along the perimeter of the heating wall, and

$$T_l(z) = \frac{\sum\sum \rho_l(i,j,k)\cdot w(i,j)\cdot C_p \cdot T_l(i,j,k)\Delta x\Delta y}{\sum\sum \rho_l(i,j,k)\cdot w(i,j)\cdot \Delta x\Delta y \cdot C_p(i,j,k)} \tag{7}$$

3. Results and discussion

Three-dimensional numerical simulations of forced convection in the microchannel under the same experimental conditions were carried out using the commercial software package "FLUENT". The sketch of the computational domain is shown in Fig. 2, where fifteen microheaters, occuping a heating area of 200 μm (width) × 30 mm (length) in size, were located between 5 and 35 mm from the entrance of the bottom wall in the microchannel.

3.1. Comparison of numerical results with experimental data

Numerical solutions were first carried out in the microchannel with 30 mm in length with partially-heated (with heating from microheater #1 only) and fully-heated (with heating from microheaters #1 to #15) Pyrex walls and the results are presented in Figs. 3 and 4, respectively. Fig. 3a and b show the wall temperature distribution and the Nusselt number for the partially heated case (with heating from microheater #1) at three effective heat fluxes of q_{eff} = 986.3 kW/m^2, 1481.6 kW/m^2, and 1974.9 kW/m^2 with T_{in} = 20 °C at various mass fluxes. Fig. 3a shows that the wall temperature decreased with increasing mass flux and decreasing heat flux as expected. Fig. 3b shows that the heat flux had a small effect on the Nusselt number because fluid properties (thermal conductivity and viscosity) were varied with temperature, which was associated with heat flux. It is noted that the Nusselt number increased with the mass flux without approaching a limit. Fig. 3c and d are comparisons of microheater temperature and the Nusselt number between numerical predication and experimental data, $T_{w,pred}/T_{w,expt}$, Nu_{pred}/Nu_{expt}, and the mean average errors (MAE) of temperature and Nusselt number measurements which are defined as:

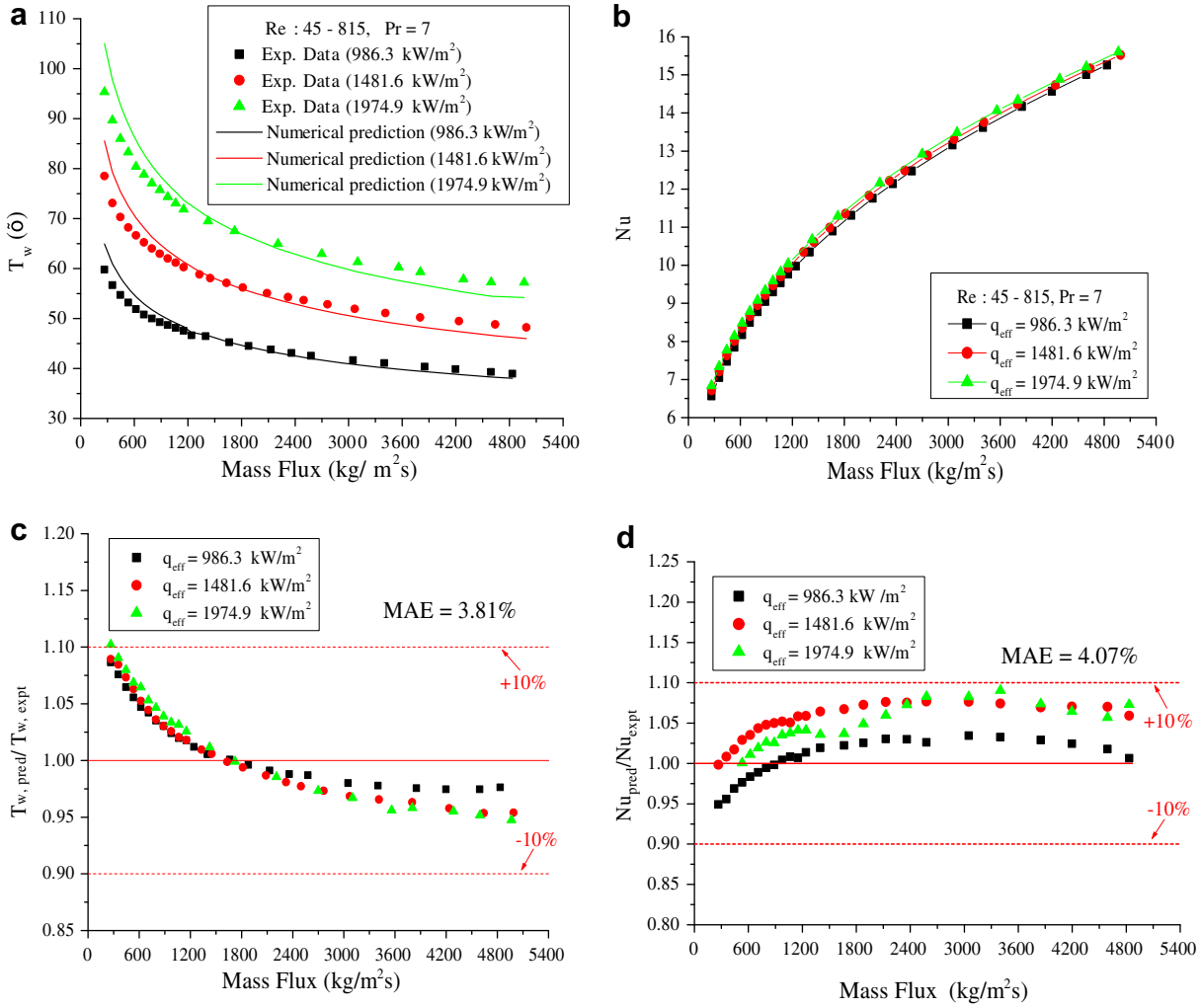

Fig. 3. Comparison of numerical predictions and experimental data for forced convection of water in a microchannel (D_h = 155 μm and L = 30 mm) with a partially heated wall. (a) Comparison of wall temperature (b) Numerical predictions of Nusselt number (c) Wall temperature ratio vs. mass flux (d) Nusselt number ratio vs. mass flux.

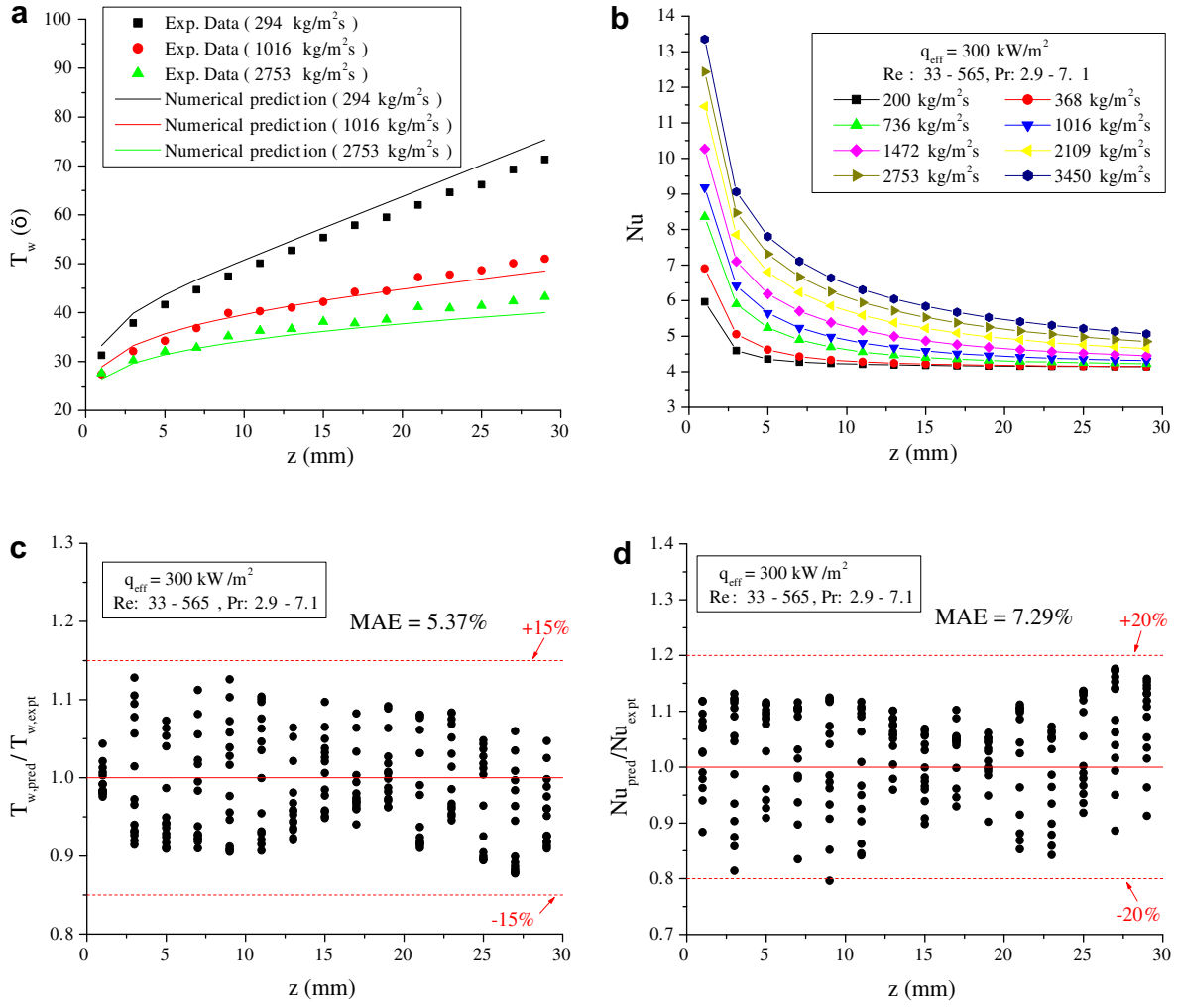

Fig. 4. Comparison of numerical predictions and experimental data for forced convection of water in a microchannel (D_h = 155 μm and L = 30 mm) with a fully-heated wall. (a) Comparison of wall temperature (b) Numerical predictions of local Nusselt number (c) Wall temperature ratio vs. distance (d) Local Nusselt number ratio vs. distance.

$$\mathrm{MAE}(T_w) = \frac{1}{M}\sum \frac{|T_{w,expt} - T_{w,pred}|}{T_{w,expt}} \times 100\% \text{ and}$$

$$\mathrm{MAE}(Nu) = \frac{1}{M}\sum \frac{|Nu_{expt} - Nu_{pred}|}{Nu_{expt}} \times 100\%, \quad (8)$$

where M is the number of data points. It can be seen from Fig. 3c and d that the numerical simulations of microheater temperature agreed well with those of experimental results with the MAE(T_w) and MAE(Nu) being 3.8% and 4.1%, respectively, for this case of a partially-heated wall. The good agreement of numerical predictions and experimental data for wall temperatures and Nusselt numbers confirmed that Navier–Stokes and energy equations are valid to model forced convection in a microchannel having a hydraulic diameter as small as 155 μm.

Numerical results for forced convection in the same microchannel with fully-heated wall (with heating from microheaters #1 to #15) at q_{eff} = 300 kW/m^2 are presented in Fig. 4. Fig. 4a and b show comparisons of numerical results and experimental data for wall temperatures and local Nusselt numbers at selected microheaters at different mass fluxes with Reynolds number ranging from 33 to 565. Fig. 4a shows that the wall temperature increased along the streamwise direction, indicating that heat was conducted from downstream part of the microheater to the front part of the microheater. Fig. 4b shows that the local Nusselt number decreased sharply from the entrance. At low mass flux, the local Nusselt number gradually approached a constant value. At high mass fluxes, however, the local Nusselt number did not approach a constant value at the channel outlet (z = 30 mm), implying that the thermal entrance length was larger than the channel heating length of 30 mm. Fig. 4c and d show that the MAE(T_w) and MAE(Nu) were 5.4% and 7.3% showing excellent agreement between numerical results and experimental data once again.

3.2. Nearly thermally fully-developed forced convection in a microchannel

As mentioned in Section 3.1, the entrance thermal length was larger than the heating length of 30 mm at high mass fluxes. In order to obtain the Nusselt number for a thermally fully-developed flow, a numerical simulation of forced convection in a fictitious microchannel with the same cross-section (as shown in Fig. 2) but with the heating length of the microchannel extended to 100 mm at q_{eff} = 100 kW/m^2 was carried out. The numerical results for the local Nusselt number versus dimensionless distance Z^+ with $Z^+ = z/(D_h \mathrm{RePr})$ is presented in Fig. 5a. It is seen that local Nusselt numbers for different mass fluxes collapsed into one curve and approached an asymptote vale of 4.00 at large values of dimensionless distance. Fig. 5b is the enlarged plot of Fig. 5a showing the

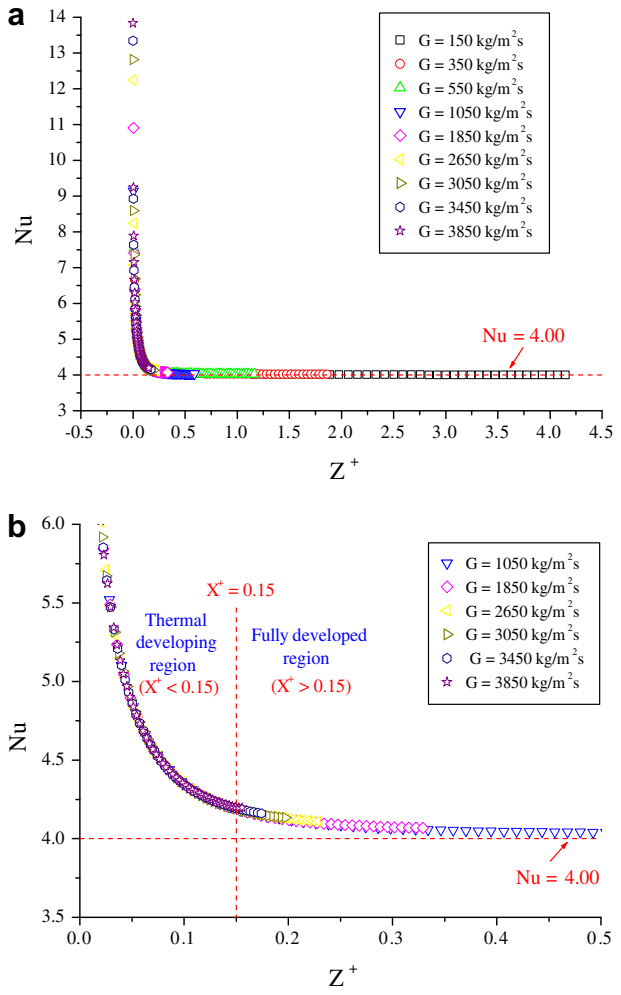

Fig. 5. Numerical results of local Nusselt number forced convection of water in a microchannel (D_h = 155 μm and L = 100 mm) with one wall fully-heated at q_{eff} = 100 kW/m^2. (a) Local Nusselt number versus dimensionless distance Z$^+$ (b) Enlarged plot of *Nu* vs. Z^+ from 0 to 0.5.

thermal developing region as well as the fully-developed region. Here, the thermal entrance length was defined as the axial distance required to achieve a value of the local Nusselt number, which was 1.05 times the fully-developed Nusselt number value. According to the numerical results, the thermal entrance length Z^+ for this case is given by $Z^+ = 0.15$, i.e., $z = 0.15 ReP r D_h$.

4. Concluding remarks

In this paper, an experiment has been carried out to study forced convection of water in a microchannel having a hydraulic diameter of 155 μm with one-wall partially and fully-heated with a length of 30 mm. Numerical simulations of wall temperature distributions and local Nusselt number corresponding to the same experimental conditions were carried out and compared with experimental data. In addition, numerical simulation was also carried out for a microchannel with the same cross-section but with the heating length extended to 100 mm. The following conclusions can be drawn from the present study: (i) The good agreement between the numerical predictions and experimental data of wall temperature distribution and the local Nusselt number confirms that classical Navier–Stokes and energy equations are still valid to model convection in microchannels having a hydraulic diameter as small as 155 μm. (ii) For forced convection in a microchannel having a trapezoidal cross-section with bottom wall heated, the numerical results show that the thermal entrance length is given by $z = 0.15 ReP r D_h$, and the fully-developed Nusselt number is approximately equal to 4.00.

Acknowledgement

This work was supported by the National Natural Science Foundation of China through Grant No. 50536010.

References

[1] D.B. Tuckerman, R.F.W. Pease, High-performance heat sinking for VLSI, IEEE Electron Device Lett. EDL-2 (1983) 126–129.
[2] X.F. Peng, G.P. Peterson, Convective heat transfer and flow friction for water flow in microchannel structures, Int. J. Heat Mass Transfer 39 (1996) 2599–2608.
[3] W.L. Qu, G.M. Mala, D.Q. Li, Heat transfer for flow water flow in trapezoidal silicon microchannels, Int. J. Heat Mass Transfer 43 (2000) 3925–3936.
[4] H.Y. Wu, P. Cheng, An experimental study of convective heat transfer in silicon microchannels with different surface conditions, Int. J. Heat Mass Transfer 46 (2003) 2547–2556.
[5] A. Weisberg, H.H. Bau, J. N Zemel, Analysis of microchannels for integrated cooling, Int. J. Heat Mass Transfer 35 (1992) 2465–2474.
[6] A.G. Fedorov, R. Viskanta, Three-dimensional conjugate heat transfer in the microchannel heat sink for electronic packaging, Int. J. Heat Mass Transfer 43 (2000) 399–415.
[7] W.L. Qu, I. Mudawar, Analysis of three-dimensional heat transfer in micro-channel heat sinks, Int. J. Heat Mass Transfer 45 (2002) 3973–3985.
[8] J. Li, G. P Peterson, P. Cheng, Three-dimensional analysis of heat transfer in a micro-heat sink with single phase flow, Int. J. Heat Mass Transfer 47 (2004) 4215–4231.
[9] G.D. Wang, P. Cheng, Subcooled flow boiling and microbubble emission boiling phenomena in a partially heated microchannel, Int. J. Heat Mass Transfer 52 (2009) 79–91.